



Improving Indoor Air Quality with Green Walls: An Experimental Study

Feliciano Falcone^{1*}, Gianluca Coccia¹, Costanzo Di Perna¹, Luca Tarabelli¹, Marco D'Orazio²,
Elisa Di Giuseppe²

¹ Department of Industrial Engineering and Mathematical Sciences, Marche Polytechnic University, Ancona 60131, Italy

² Department of Civil, Building and Architecture Engineering, Marche Polytechnic University, Ancona 60131, Italy

Corresponding Author Email: f.falcone@pm.univpm.it

Copyright: ©2025 The authors. This article is published by IETA and is licensed under the CC BY 4.0 license
(<http://creativecommons.org/licenses/by/4.0/>).

<https://doi.org/10.18280/ijstdp.201002>

ABSTRACT

Received: 7 August 2025

Revised: 14 September 2025

Accepted: 24 September 2025

Available online: 31 October 2025

Keywords:

*air change rate, CO₂ removal, indoor air
quality (IAQ), living wall, passive air
purification*

Poor indoor air quality (IAQ), particularly elevated CO₂ concentrations, is known to impair cognitive function and comfort. In sealed or energy-efficient buildings, natural air exchange is limited, increasing the need for passive pollutant removal strategies. This study evaluates the CO₂ removal capacity of a living wall system installed in a full-scale climatic chamber (38 m³). Controlled CO₂ decay tests were performed under two conditions: with LED illumination (photosynthesis active) and without lighting. The temporal evolution of CO₂ concentration was modeled using a first-order exponential decay function, and equivalent air change rates (ACH_e) were calculated. Under illumination, the half-life of CO₂ decreased from 90 to 63 minutes (-30%), with an additional removal of approximately 6 g of CO₂ over 6 hours. The ACH_e increased from 0.46 h⁻¹ (LED OFF) to 0.66 h⁻¹ (LED ON), representing a 43% improvement in effective air renewal attributable to photosynthesis. The findings confirm the synergistic role of lighting and vegetation in enhancing passive indoor air purification. Properly illuminated living walls (LWs) can achieve substantial CO₂ removal rates, offering a sustainable strategy for improving IAQ in energy-efficient buildings.

1. INTRODUCTION

Indoor air quality (IAQ) is critical to health, especially in indoor environments such as schools and offices [1]. Since people spend up to 90% [2] of their time indoors, it is essential to monitor and improve IAQ to prevent adverse health effects [3, 4]. There is a well-documented correlation between air quality and thermohydrometric comfort, with the impact on both physical and psychological well-being [5]. Stagnant or odorous air impairs well-being [6], causing discomfort, headaches, and irritation, and reduces perceived comfort even when temperature and humidity are optimal [7]. Carbon dioxide (CO₂) is a frequently employed tracer gas in the assessment of air exchange and the accumulation of pollutants in indoor environments [8]. Controlled mechanical ventilation (CMV) remains the standard for IAQ control, but it is energy-intensive and often does not respond to changes in occupancy or pollutant loads [9]. In energy-efficient buildings, reduced natural ventilation increases the risk of indoor pollution accumulation [10]. The impacts on health and the economy are significant, with estimated social costs of up to €20 billion per year [11]. In addition, CMV systems face rising costs due to energy prices, complex maintenance, and the need for advanced technologies [12], which is driving the search for sustainable alternatives. To improve indoor environmental quality, integrating vertical vegetated structures—Green Walls (GWs)—offers a sustainable, nature-based solution. Their vertical layout maximizes vegetated area with minimal

floor space and adds both pollutant reduction and psychological benefits [13]. GWs include green facades, which use climbing plants, and living walls (LWs), which consist of pre-grown plants on panels with artificial irrigation and nutrient systems [14]. LWs, though effective, are maintenance-intensive, especially indoors where light, rain, and ventilation are limited, requiring artificial lighting, drainage, and controlled irrigation. In this context, some studies have focused specifically on the ability of LW to remove CO₂ in controlled environments, evaluating the role of factors such as lighting, and plant type. Dominici et al. [15] showed that optimized lighting (200 μmol · m⁻² · s⁻¹ at 15°) significantly enhances CO₂ uptake in passive green walls, achieving an equivalent air exchange rate of 0.21 h⁻¹ in a 40 m³ office. Under typical indoor lighting (≤ 50 μmol · m⁻² · s⁻¹), performance drops sharply to just 0.03 h⁻¹. Danielski et al. [16] studied two Swedish classrooms equipped with 310 plants and found a 10% CO₂ reduction during school hours (~70 ppm), a 0.8°C rise in indoor temperature with greater thermal stability, and up to 18% annual heating energy savings with reduced ventilation. The study also reported improved student well-being, including reduced stress.

Despite numerous studies, quantitative data usable for experimental validation or simulation remains limited. To address this gap, we conducted tests in a full-scale climate chamber equipped with two vertical LW, comparing CO₂ decay under two conditions: with and without artificial LED lighting (LED ON, and OFF). Concentration was measured

over time with point sensors and fitted using a first-order exponential decay model. A Random Search Method (RSM) was used to estimate decay constants for both cases. Unlike previous small-scale or theoretical studies, this work provides high-resolution data in a thermally controlled environment, enabling quantification of both instantaneous and cumulative photosynthetic effects. The integration of the two fitted curves allows estimation of the net CO₂ removal due to lighting, showing a 30% reduction in half-life and an additional 6 g of CO₂ absorbed in 6 hours. These findings support the synergy between lighting and vegetation for IAQ control.

The present work is organized as follows: Section 2 Materials and Methods provides an overview of the climatic chamber used for testing and the measurement methodology used. The results of the tests carried out are given in Section 3. Finally, the conclusions and future developments of the work are presented in Section 4.

2. MATERIALS AND METHODS

This section describes the climate chamber employed for experimental procedures and provides a detailed description of

the measurement methodology adopted in this paper.

2.1 Climate chamber and living wall

The experimental tests were conducted within a full-scale climate chamber ($4.3 \times 3.3 \times 2.7$ m) located in the Environmental Energy Laboratory of Marche Polytechnic University (Ancona, Italy). The chamber features insulated mineral fiber panels (thickness of 0.45 m) and is elevated above the lab floor (~ 0.30 m). The configuration of the climate chamber is depicted in its plan view (Figure 1). Two fabric panels (1.35×2.35 m, ~ 127 kg per panel) were installed on one vertical wall, for a total vegetated area of 6.34 m². The panels incorporate pockets filled with rock wool soaked in natural fertilizers, ensuring good aeration and moisture distribution. Each panel is divided into upper and lower zones with independent irrigation: dual lines supply 1.75 L/s for 50 min every other day to the upper zone, while a single line supplies 1.0 L/s for 25 min to the lower zone. Excess water is drained into an external tank via a channel at the base. This ensures that the soil moisture content remains within the optimal range between 25 and 35%, thereby facilitating the growth of the plants.

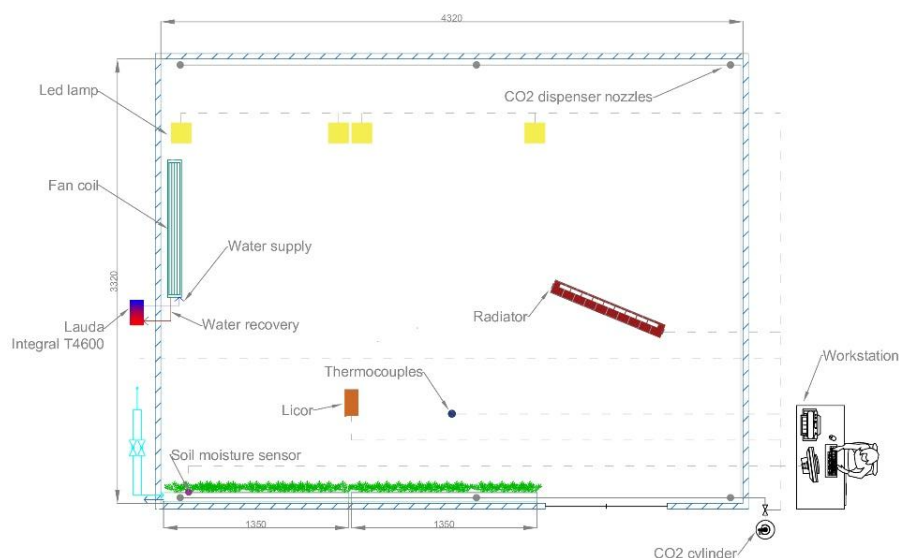


Figure 1. Plan view of the climate chamber. The main elements (sensors, lamps, workstation, etc.) are highlighted



Figure 2. Installed LWs in climate chamber

Three different plant species were chosen (see Figure 2). *Spathiphyllum* (i.e., Peace Lily) and *Ficus Pumila Green Sunny* cover the upper and lower areas of the left LW. *Schefflera Arboricola Janine* and *Epipremnum Pinnatum Aureum* (i.e., Pothos) cover the upper and lower areas of the right LW.

Since LW systems allow for the development of aesthetic GW solutions, the variety of plants was chosen for their diversity in terms of leaf shape, texture, color, density and presence of flowers.

2.2 Monitoring techniques

This section comprises information regarding the monitoring techniques utilized in the present study. The analysis will focus on the following parameters: temperature, illumination, air humidity and carbon dioxide concentration.

2.2.1 Temperature measurements and control

Temperature was monitored using 28 type T thermocouples ($\pm 0.5^\circ\text{C}$, 0.1 Hz), 20 suspended at a height of 1.7 m and 8 mounted on a vertical pole to detect the vertical profile. In the LED ON configuration, approximately 10% of the electrical energy absorbed was converted into heat. This required, as shown in Figure 1, the development of a controlled system consisting of a radiator and a fan coil unit, connected to an external thermostatic bath (Lauda Integral T 4600). As shown in Figure 3, the temperature initially increased during system heating, then stabilized (is raised to $20^\circ\text{C} \pm 0.5^\circ\text{C}$) after the fan coil unit was activated. The fan coil-radiator combination allows the average temperature to remain constant over time.

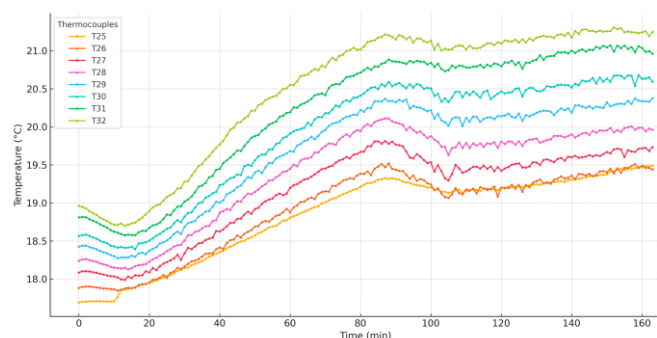


Figure 3. Temperature trend over time measured by the eight thermocouples (T25-T32) mounted on the vertical pole inside the climate chamber

2.2.2 Illumination measurements

In the presence of light, plants within the climate chamber undergo photosynthesis, during which carbon dioxide (CO_2) is absorbed from the surrounding air and converted into glucose and oxygen. The rate of CO_2 absorption is directly influenced by the availability of light, which drives the light-dependent reactions of photosynthesis. To promote optimal conditions for the photosynthesis process, four LED lamps emitting light within the 400-700 nm range (visible light) were installed within the climate chamber. As demonstrated in Figure 4, the lamps are positioned at the extremities of both panels, at approximately 3 m from the LWs. It has been demonstrated (Figure 4) that this facilitates a Photosynthetically Active Radiation (PAR) range of 50 to $110 \mu\text{mol} \cdot \text{m}^{-2} \cdot \text{s}^{-1}$ in proximity of the LWs themselves.

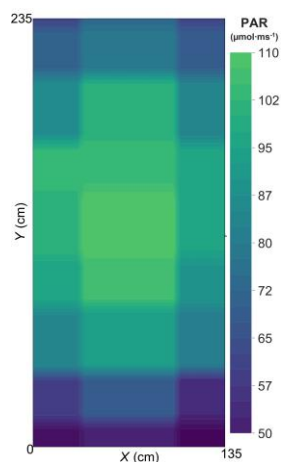


Figure 4. Spatial distribution of PAR measured (mean value) at canopy level for each LW

2.2.3 CO_2 and air humidity measurements

CO_2 and humidity were monitored using a Licor LI-7815 analyzer, based on OF-CEAS technology (1 Hz, ± 0.10 ppm for CO_2 , ± 45 ppm for humidity). Relative humidity was derived from water vapor concentration (ppm). The sensor was placed at 1.5 m height, between the two LWs (Figure 1). After stabilizing the chamber temperature at $24^\circ\text{C} (\pm 0.5^\circ\text{C})$, CO_2 was injected from an external cylinder via six ceiling-mounted nozzles. The target concentration (3000 ppm) was calculated using the ideal gas law [17], based on the chamber volume, initial CO_2 , and temperature. Injection followed alternating 30 s pulses and 90 s pauses to ensure homogeneous mixing. After the injection phase, the decay of CO_2 over time was observed with the Licor sensor: the test was considered completed when the CO_2 concentration in the room returned to 500 ppm. The decay was observed under the two conditions (LED ON, and OFF).

3. RESULTS

This section presents and discusses the results of the tests carried out in the present work. The experimental procedure was conducted under controlled temperature conditions of $24^\circ\text{C} (\pm 0.5^\circ\text{C})$.

3.1 Experimental decay curves

To assess the reproducibility of the experimental setup, three independent tests under LED OFF conditions were analyzed. As shown in Figure 5, the decay curves obtained in LED OFF mode are similar. The mean standard deviation σ among the three tests was 9.28 ppm: this confirms the high degree of repeatability and consistency of the measurements across different trials. The maximum decay time was about 800 min, the minimum 740 min. Table 1 presents the CO_2 decay profiles recorded during the tests. The initial reading, taken at the commencement of the experiment, indicated an approximate concentration of 3020 ppm. Over the course of the 800-minute test period, there was a consistent decrease in concentration, reaching a final average of 502 ppm. Looking at Figure 5 and Table 1, the decay exhibited across all three replicates is characterized by a smooth and progressive decline, with a more rapid decrease during the initial 180 minutes, followed by a gradual stabilization. It is noteworthy that a high degree of consistency is observed between the three trials. At each point, the measured values are closely aligned, with only minor deviations.

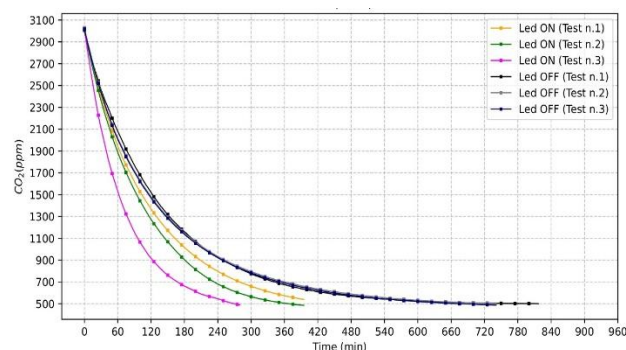


Figure 5. Experimental decay curves for the condition LED ON/OFF ($24^\circ\text{C} \pm 0.5^\circ\text{C}$)

This phenomenon is reflected in the average column, which closely follows each individual dataset. The low spread observed across the three series is indicative of the high reproducibility of the experimental setup.

Figure 5 also presents the CO₂ concentration decay profiles under LED ON conditions for three independent tests. The curves are color-coded as follows: orange (Test 1), green (Test 2), and magenta (Test 3).

It is evident that all three curves demonstrate the characteristic exponential decay behavior.

Despite the general similarity in shape, the decay rates vary between the three tests. It is noteworthy that Test 3 (magenta) exhibited the most rapid reduction, achieving values below 600 ppm in less than 300 minutes. In contrast, Test 1 (orange) displays a slower decay, while Test 2 (green) presents an intermediate trend. These differences can be attributed to the increasing leaf area of the plants across the successive tests. As the plants grew, their photosynthetic capacity improved, leading to higher rates of CO₂ absorption. This phenomenon is especially pronounced in the steeper decline observed in Test 3. Table 2 provides numerical confirmation of these observations. At each point, the CO₂ concentrations recorded in Test 3 are lower than those in Tests 1 and 2. For instance, following 180 minutes of operation, the concentration in Test 3 is recorded as 657 ppm, in comparison to 1006 ppm and 893 ppm in Tests 1 and 2, respectively. The mean values derived from the three tests demonstrate this trend, exhibiting a progressive decline that corresponds to the physiological development of plants.

A comparison between the CO₂ decay profiles under LED OFF and LED ON conditions reveals substantial differences in the dynamics of concentration reduction. In all cases, the presence of illumination leads to a more rapid decrease in CO₂ levels, consistent with the activation of photosynthetic mechanisms.

The findings of the individual tests demonstrate that the rate of decay is significantly increased under the influence of light. For instance, following 180 minutes of operation, the CO₂ concentrations in the LED ON tests ranged from 657 to 1006 ppm, while the LED OFF tests exhibited higher concentrations, ranging from 1128 to 1150 ppm (Tables 1, 2). This discrepancy becomes increasingly evident over time. The divergence between the two conditions manifests at the outset and becomes more pronounced as time progresses. Following a period of 60 minutes, the mean concentration of the substance under the condition of LED ON was found to be 1788 ppm, whereas under the condition of LED OFF it remained at 2034 ppm, a discrepancy of 249 ppm (-12%). This discrepancy is found to widen progressively: after 180 minutes, the LED ON condition shows an average of 852.01 ppm, compared to 1139.24 ppm in the LED OFF scenario, resulting in a delta of 287.2 ppm (-25%).

As demonstrated in Tables 1 and 2, the difference in mean CO₂ concentration stabilizes at 300 minutes, with an average of 667.54 ppm when lighting is operational, and 776.08 ppm in the absence of lighting. This indicates a persistent difference of 108.5 ppm. This finding suggests that the most significant separation occurs within the initial 3 - 4 hours, coinciding with the period when the plants' photosynthetic activity is at its peak relative to the background decay. The implementation of artificial illumination not only speeds up CO₂ removal but also reduces the residual concentration level towards which the system tends to converge. This outcome is consistent with the anticipated effect of elevated CO₂ uptake by the plants, a

consequence of the stimulation of photosynthetic activity by the LED lighting.

Table 1. Evolution of CO₂ concentration (ppm) over time (min) under experimental conditions (24°C ± 0.5°C) with LED illumination off (LED OFF)

| LED OFF | | | | |
|------------|--------------|--------------|--------------|------------|
| Time (min) | Test 1 (ppm) | Test 2 (ppm) | Test 3 (ppm) | Avg. (ppm) |
| 0 | 3012 | 3031 | 3019 | 3020 |
| 60 | 2079 | 2017 | 2005 | 2033 |
| 120 | 1513 | 1473 | 1461 | 1482 |
| 180 | 1150 | 1140 | 1128 | 1139 |
| 240 | 921 | 926 | 914 | 920 |
| 300 | 766 | 787 | 775 | 776 |
| 360 | 667 | 694 | 682 | 681 |
| 420 | 604 | 631 | 619 | 618 |
| 480 | 567 | 585 | 573 | 575 |
| 540 | 541 | 552 | 540 | 544 |
| 600 | 523 | 529 | 517 | 523 |
| 700 | 506 | 505 | 493 | 506 |
| 800 | 501 | | | 501 |

Table 2. Evolution of CO₂ concentration (ppm) over time (min) under experimental conditions (24°C ± 0.5°C) with LED illumination on (LED ON)

| LED ON | | | | |
|------------|--------------|--------------|--------------|------------|
| Time (min) | Test 1 (ppm) | Test 2 (ppm) | Test 3 (ppm) | Avg. (ppm) |
| 0 | 3006 | 3004 | 3019 | 3009 |
| 60 | 1946 | 1887 | 1531 | 1788 |
| 120 | 1360 | 1265 | 910 | 1178 |
| 180 | 1006 | 893 | 657 | 852 |
| 240 | 789 | 673 | 541 | 667 |
| 300 | 653 | 559 | 501 | 571 |
| 360 | 568 | 502 | | 534 |
| 420 | 503 | | | 502 |

3.2 Model fitting of CO₂ decay

This analysis aims to model the decay of CO₂ concentration over time within a confined environment under the two conditions (LED ON, and OFF).

The behavior of indoor CO₂ concentration in the absence of significant new emissions can be described by an exponential decay model [9]. The simplest form [10] of this model is:

$$C(t) = C_0 \cdot e^{-k \cdot t} \quad (1)$$

where, $C(t)$ is concentration (ppm) at time t (min), C_0 is initial concentration (ppm) and k is decay coefficient (min⁻¹). However, the curves in Figure 5 show a minimum concentration limit value (approximately 500 ppm), so the model in Eq. (1) can be evaluated [10]:

$$C(t) = C_{\infty} + (C_0 - C_{\infty}) \cdot e^{-k \cdot t} \quad (2)$$

where, C_{∞} is the asymptotic concentration.

The analysis was conducted using the Random Search Method (RSM) [18], which allows parameter estimation and minimizing the average absolute relative deviation (AARD) between the experimental values and the model. The initial value was kept fixed at the mean value at time t_0 .

AARD($C(t)$) [19] is expressed as:

$$AARD(C(t)) = \frac{100}{N} \sum_{i=1}^N \left| \frac{C(t)_{calc} - C(t)_{exp}}{C(t)_{exp}} \right| \quad (3)$$

where, N is the number of experimental points, $C(t)_{calc}$ and $C(t)_{exp}$ are the calculated and the experimental concentration value respectively.

Fitting was conducted separately for each condition imposing lower and upper bounds to ensure numerical stability.

The following equations are derived from the analysis:

$$C_{ON}(t) = 474.6 + 2534.8 \cdot e^{-0.011 \cdot t} \quad (4)$$

$$C_{OFF}(t) = 511.2 + 2509.5 \cdot e^{-0.007 \cdot t} \quad (5)$$

The equations demonstrate an AARD (%) of 1.2% for Eq. (4) and 2.4% for Eq. (5). It is evident that both models demonstrate a high degree of accuracy. The estimated values of the decay constant k highlight a clear difference between the two experimental conditions. Under LED ON, the decay rate was $k = 0.011 \text{ min}^{-1}$, while under LED OFF it was $k = 0.007 \text{ min}^{-1}$. This corresponds to a relative increase of approximately 45% in the presence of illumination, indicating that CO_2 is removed more rapidly when photosynthetic activity is stimulated by light.

To better interpret this result, the half-life time τ , defined as the time required for the CO_2 concentration to reduce to half of its initial excess, is computed as [20]:

$$\tau = \frac{\ln(2)}{k} \quad (6)$$

Accordingly, the half-life under LED OFF conditions increases to 90 minutes, while under LED ON conditions is approximately 63 minutes (-30%). This substantial reduction in $t_{1/2}$ confirms that the presence of artificial lighting

significantly accelerates the decay of CO_2 concentrations. To facilitate comparison with mechanical ventilation, the decay constants were converted into equivalent air change rates (ACH_e) using $\text{ACH}_e = k \cdot 60$, assuming a well-mixed volume [10]. The resulting values are 0.46 h^{-1} (LED OFF) and 0.66 h^{-1} (LED ON), indicating a marked increase (43%) in effective air renewal due to photosynthetic activity. The system responds more efficiently to CO_2 accumulation, leading to faster improvements in IAQ when illumination is provided. As illustrated in Figure 6, the decay curves are depicted as a function of time, under LED ON, and OFF conditions. The solid curve denotes the mean values derived from the experimental data points, while the dashed curve signifies the calculated curves. To quantitatively assess the cumulative impact of artificial lighting on CO_2 removal, the area between the two model curves was computed.

This area, shown in gray in Figure 6, represents the integral overtime difference between the two scenarios:

$$A = \int_0^{360} (C_{OFF}(t) - C_{ON}(t)) dt \quad (7)$$

The integration was performed over the interval from 0 to 360 minutes and was computed numerically using the trapezoidal rule [21], which approximates the area under a curve by summing up the areas of trapezoids formed between adjacent points of the fitted model curves. The result is approximately $86'515 \text{ ppm} \cdot \text{min}$, which quantifies the excess CO_2 that accumulates in the absence of illumination: It reflects the cumulative exposure to higher CO_2 levels under LED OFF conditions. Although not directly a mass, this integral is proportional to the total amount of CO_2 retained, and—when multiplied by the room volume and an appropriate conversion factor—allows for estimation of the effective mass removed. In this case, the difference corresponds to an estimated 6.06 grams of CO_2 removed more efficiently when lights were on.

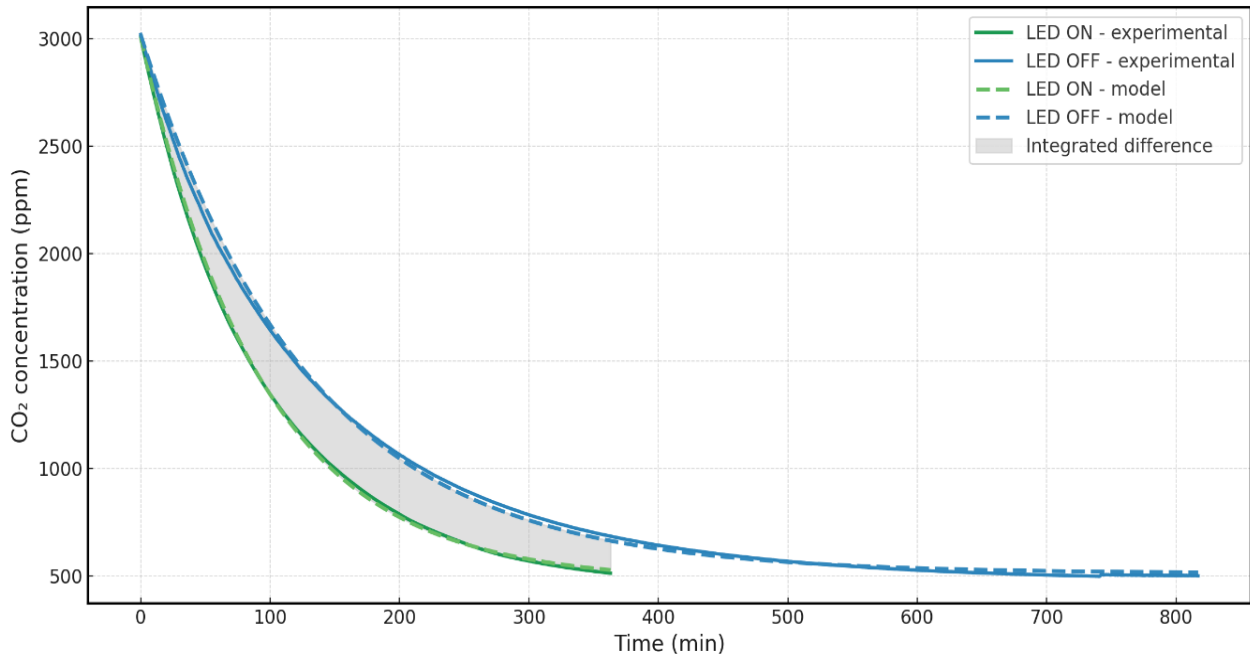


Figure 6. Comparison between experimental and fitted CO_2 decay curves under LED ON and LED OFF conditions. The shaded area highlights the integrated concentration difference between the two scenarios, calculated over the first 360 minutes

4. CONCLUSIONS

The present study investigated the temporal decay of CO₂ concentrations in a controlled climate chamber.

The experimental campaign was conducted at $24 \pm 0.5^\circ\text{C}$ under LED ON/OFF conditions. The findings demonstrated that the presence of illumination significantly accelerates the process of CO₂ removal from indoor air. Decay curves revealed a clear exponential trend, which was modelled using a first-order decay equation with an asymptotic minimum. The Random Search Method was utilized to calibrate the decay constants under both conditions, thereby confirming a higher decay rate under illumination. In particular, the half-life of the CO₂ concentration was found to decrease from approximately 90 minutes (LED OFF) to 63 minutes (LED ON), representing a 30% reduction. This finding suggests that the system exhibits a more rapid dynamic response when photosynthesis is initiated by light. The cumulative impact of lighting was further quantified by calculating the area between the model curves. Over the initial 360 minutes, the integrated difference amounted to 86'515 ppm·min, corresponding to an estimated 6.06 grams of CO₂ additionally removed when lighting was active. Furthermore, the decay constants were translated into ACH_e, yielding values of 0.46 h⁻¹ without lighting and 0.66 h⁻¹ with lighting. This corresponds to a 43% increase in effective air renewal due to the activation of photosynthetic processes. The findings support the role of vegetated systems in enhancing IAQ and highlight how controlled lighting can actively contribute to accelerating pollutant removal through biological processes. The results provide quantitative evidence of the synergy between artificial lighting and living walls, which can inform energy-efficient strategies for indoor environmental management.

It is important to note, however, that the results are specific to the experimental conditions reported and should be interpreted accordingly. The conclusions refer to a single chamber configuration with a defined plant species, light spectrum, and constant temperature. While the trends are clear and quantitatively relevant, the findings represent a partial view limited to the tested setup and are not intended to be generalized to all indoor environments or green wall typologies without further validation. As such, the generalizability of the results to other indoor environments may be constrained, especially in the presence of external ventilation, dynamic occupancy, or varying climatic conditions.

Future work will aim to extend the methodology to multiple environmental configurations, including different temperatures, humidity levels, and light spectra. The integration of real-time CO₂ monitoring with adaptive lighting strategies is also foreseen, with the goal of developing intelligent, plant-responsive indoor environmental systems. Additionally, combining passive plant systems with mechanical ventilation could offer hybrid IAQ management strategies. Long-term testing on diverse plant species will further clarify the biological mechanisms and performance variability of living walls under real-world conditions.

ACKNOWLEDGMENT

We would like to thank the company Pellegrini Giardini, and in particular Dr. A. Pellegrini and P. Curini, for providing the species of the living wall along with some of experimental

systems used for testing, and for their valuable support during the whole experimental campaign. The authors would also like to thank F. Tartaglini for his support during the mounting of the experimental set-up.

REFERENCES

- [1] Chiesa, G., Vigliotti, M. (2024). Comparing mechanical ventilation control strategies for indoor air quality: Monitoring and simulation results of a school building in northern Italy. *Energy and Buildings*, 322: 114665. <https://doi.org/10.1016/j.enbuild.2024.114665>
- [2] Mata, T.M., Martins, A.A., Calheiros, C.S.C., Villanueva, F., Alonso-Cuevilla, N.P., Gabriel, M.F., Silva, G.V. (2022). Indoor air quality: A review of cleaning technologies. *Environments*, 9(9): 118. <https://doi.org/10.3390/environments9090118>
- [3] Andualet, Z., Gizaw, Z., Bogale, L., Dagne, H. (2019). Indoor bacterial load and its correlation to physical indoor air quality parameters in public primary schools. *Multidiscip Respir Med*, 14: 2. <https://doi.org/10.1186/s40248-018-0167-y>
- [4] Klepeis, N.E., Nelson, W.C., Ott, W.R., Robinson, J.P., Tsang, A.M., Switzer, P., Behar, J.V., Hern, S.C., Engelmann, W.H. (2001). The national human activity pattern survey (NHAPS): A resource for assessing exposure to environmental pollutants. *Journal of Exposure Analysis and Environmental Epidemiology*, 11(3): 231-252. <https://doi.org/10.1038/sj.jea.7500165>
- [5] Sivarethinamohan, R., Sujatha, S., Priya, S., Sankaran, Gafoor, A., Rahman, Z. (2021). Impact of air pollution in health and socio-economic aspects: Review on future approach. *Materials Today: Proceedings*, 37: 2725-2729. <https://doi.org/10.1016/j.matpr.2020.08.540>
- [6] Navarrete-Meneses, M.P., Salas-Labadía, C., Gómez-Chávez, F., Pérez-Vera, P. (2024). Environmental pollution and risk of childhood cancer: A scoping review of evidence from the last decade. *International Journal of Molecular Sciences*, 25(6): 3284. <https://doi.org/10.3390/ijms25063284>
- [7] Zhao, D., Azimi, P., Stephens, B. (2015). Evaluating the long-term health and economic impacts of central residential air filtration for reducing premature mortality associated with indoor fine particulate matter (PM_{2.5}) of outdoor origin. *International Journal of Environmental Research and Public Health*, 12(7): 8448-8479. <https://doi.org/10.3390/ijerph120708448>
- [8] Cincinelli, A., Martellini, T. (2017). Indoor air quality and health. *International Journal of Environmental Research and Public Health*, 14(11): 1286. <https://doi.org/10.3390/ijerph14111286>
- [9] Persily, A. K. (2015). Field measurement of ventilation rates. *Indoor Air*, 26(1): 97-111. <https://doi.org/10.1111/ina.12193>
- [10] Etheridge, D., Sandberg, M. (1996). *Building Ventilation: Theory and Measurement*. Chichester: Wiley.
- [11] Boulanger, G., Bayeux, T., Mandin, C., Kirchner, S., Vergriette, B., Pernelet-Joly, V., Kopp, P. (2017). Socio-economic costs of indoor air pollution: A tentative estimation for some pollutants of health interest in France. *Environment International*, 104: 14-24. <https://doi.org/10.1016/j.envint.2017.03.025>

- [12] Cox, C.E., Carson, S.S., Govert, J.A., Chelluri, L., Sanders, G.D. (2007). An economic evaluation of prolonged mechanical ventilation. *Critical Care Medicine*, 35(8): 1918-1927. <https://doi.org/10.1097/01.ccm.0000275391.35834.10>
- [13] Yao, W., Zhang, X., Gong, Q. (2021). The effect of exposure to the natural environment on stress reduction: A meta-analysis. *Urban Forestry & Urban Greening*, 57: 126932. <https://doi.org/10.1016/j.ufug.2020.126932>
- [14] Radić, M., Brković Dodig, M., Auer, T. (2019). Green facades and living walls—A review establishing the classification of construction types and mapping the benefits. *Sustainability*, 11(17): 4579. <https://doi.org/10.3390/su11174579>
- [15] Dominici, L., Fleck, R., Gill, R.L., Pettit, T.J., Irga, P.J., Comino, E., Torpy, F.R. (2021). Analysis of lighting conditions of indoor living walls: Effects on CO₂ removal. *Journal of Building Engineering*, 44: 102961. <https://doi.org/10.1016/j.jobe.2021.102961>
- [16] Danielski, I., Svensson, Å., Weimer, K., Lorentzen, L., Warne, M. (2022). Effects of green plants on the indoor environment and wellbeing in classrooms—A case study in a Swedish school. *Sustainability*, 14(7): 3777. <https://doi.org/10.3390/su14073777>
- [17] Cesini, G., Polonara, F., Latini, G. (2014). *Fisica Tecnica*. Milan: McGraw-Hill Education.
- [18] Andradóttir, S. (2005). An overview of simulation optimization via random search. In *Handbooks in Operations Research and Management Science*, pp. 617-631. [https://doi.org/10.1016/S0927-0507\(06\)13020-0](https://doi.org/10.1016/S0927-0507(06)13020-0)
- [19] Seader, J.D., Henley, E.J., Roper, D.K. (2011). *Separation Process Principles*, 3rd ed. Wiley.
- [20] Levenspiel, O. (1998). *Chemical Reaction Engineering*. John Wiley & Sons.
- [21] Burden, R.L., Faires, J.D. (2011). *Numerical Analysis*, 9th ed. Boston: Brooks/Cole, Cengage Learning.

NOMENCLATURE

| | |
|-----------------------------------|--|
| AARD | Average absolute relative deviation, % |
| A | Integral, ppm · min |
| ACH _e | Equivalent air change rate, h ⁻¹ |
| C(t) | CO ₂ concentration at time t, ppm |
| C ₀ | Initial CO ₂ concentration, ppm |
| C _∞ | Asymptotic CO ₂ concentration, ppm |
| CO ₂ | Carbon dioxide |
| H ₂ O _(ppm) | Water vapor concentration, ppm |
| m | Mass of removed CO ₂ , g |
| OF-CEAS | Optical feedback - cavity enhanced absorption spectroscopy |
| PAR | Photosynthetically active radiation, μmol·m ⁻² ·s ⁻¹ |
| P | Pressure, Pa |
| R | Universal gas constant, J · mol ⁻¹ · K ⁻¹ |
| RH | Relative humidity, % |
| RSM | Random Search Method |
| k | Decay coefficient, min ⁻¹ |
| T | Air temperature, °C or K |
| t | Time, min |
| x | Water vapor mass mixing ratio, kg _v kg _a ⁻¹ |
| V | Volume, m ³ |

Greek symbols

| | |
|---|--------------------------|
| σ | Standard deviations, ppm |
| τ | Half-life time, min |

Subscripts

| | |
|------|--------------|
| a | Air |
| calc | Calculated |
| On | Led on |
| Off | Led off |
| e | Equivalent |
| Exp | Experimental |
| v | Vapor |
| sat | Satur |